Journal of Solid State Chemistry 187 (2012) 195–199

Contents lists available at SciVerse ScienceDirect

Journal of Solid State Chemistry

journal homepage: www.elsevier.com/locate/jssc

In-situ non-ambient X-ray diffraction studies of indium tungstate

Tamam I. Baiz [1], Christophe P. Heinrich [2], Nathan A. Banek [3], Boris L. Vivekens, Cora Lind *

Department of Chemistry, The University of Toledo, Toledo, OH 43606, USA

ARTICLE INFO

Article history:
Received 6 October 2011
Received in revised form
2 January 2012
Accepted 9 January 2012
Available online 18 January 2012

Keywords:
Non-hydrolytic sol-gel process
Negative thermal expansion
Indium tungstate
X-ray diffraction
Variable temperature studies
High pressure studies

ABSTRACT

In situ variable temperature and high pressure X-ray diffraction studies were carried out on indium tungstate ($In_2W_3O_{12}$). This material displays positive volume expansion in both its low temperature monoclinic and high temperature orthorhombic phases, with negative thermal expansion along the *a* axis and positive thermal expansion along the *b* and *c* axes. Upon hydrostatic compression in a diamond anvil cell, one crystalline to crystalline phase transition is observed in the range 1.9 to 2.7 GPa, and progressive irreversible amorphization occurs at pressures above 4.3 GPa. The crystalline high pressure phase appears to be isostructural to previously observed high pressure phases in other $A_2M_3O_{12}$ compounds.

1. Introduction

In recent years, there has been an increased interest in negative thermal expansion (NTE) materials, which contract upon heating [1–17]. Materials exhibiting this property have the potential for achieving better control of thermal expansion through the synthesis of composite materials with tunable expansion coefficients. A family of materials that has been known to show NTE are $A_2M_3O_{12}$ compounds, where A can be a variety of trivalent cations ranging in size from Al^{3+} to Gd^{3+}, and M can be Mo or W [16,17]. These compounds adopt two closely related crystal structures, a denser monoclinic phase in space group $P\ 2_1/a$, and an orthorhombic phase in space group Pnca [18]. Many compositions show a reversible phase transition from the monoclinic structure at low temperatures to the orthorhombic polymorph at high temperatures. The temperature of this phase transition depends on the metals incorporated into the structure [16,19–26]. NTE behavior is only observed in the orthorhombic phase.

A common feature of NTE materials is that they possess a highly flexible, corner-sharing polyhedral framework, which allows for the concerted tilting motions of the MO_x polyhedra that cause the observed expansion behavior [14,15,24]. The potential use of NTE materials as fillers in controlled expansion composites therefore necessitates investigation of their high pressure behavior, as the open framework structures make these compounds prone to pressure-induced phase transitions. Composite preparation often requires hot or cold pressing, and localized microstrain on the filler particles can result from expansion of the matrix. Pressure-induced changes in the structure of the NTE filler are detrimental to the performance of a composite [27–29], as the high pressure phases are unlikely to exhibit NTE [30]. Irreversible phase transitions will be problematic regardless of when they occur, while reversible phase transitions during composite preparation may be tolerable if the microstrain during thermal cycling does not reach the phase transition pressure.

High pressure studies on a number of NTE materials have been carried out by *in situ* diffraction experiments and Raman spectroscopy [30–35]. While Raman experiments give insights into phase transition pressures and reversibility, diffraction experiments give detailed structural information, and allow direct comparison of high pressure patterns observed for different materials. Pressure-induced phase transitions, as well as pressure-induced amorphization, have been observed in a number of NTE materials, including several $A_2M_3O_{12}$ compounds [21,34–37]. For several orthorhombic materials, a transition to the denser monoclinic phase adopted by many $A_2M_3O_{12}$ materials was observed at very low pressures ($Sc_2Mo_3O_{12}$: 0.25 GPa, $Sc_2W_3O_{12}$: 0.3 GPa, $Al_2W_3O_{12}$: 0.1 GPa) [34–37].

Indium tungstate has been previously synthesized, and its temperature-dependent behavior has been studied using diffraction,

* Corresponding author. Fax: +1 419 530 4033.
E-mail address: cora.lind@utoledo.edu (C. Lind).
[1] Present address: Science Department, Mercy College of Ohio, Toledo, OH 43604, USA.
[2] Present address: Institute of Inorganic and Analytical Chemistry, Johannes Gutenberg University Mainz, Germany.
[3] Present address: Department of Chemistry, Corcoran Hall, 725 21st Street, NW, Washington, DC 20052, USA.

0022-4596/$ - see front matter © 2012 Elsevier Inc. All rights reserved.
doi:10.1016/j.jssc.2012.01.019

differential scanning calorimetry, dilatometry and Raman spectroscopy [16,17,24,38]. A phase transition from the monoclinic $P\,2_1/a$ to the orthorhombic Pnca phase was observed at about 250 °C. Previously reported values for the linear expansion coefficient α_l were obtained by dilatometry, and range from $-3.0\times10^{-6}\,K^{-1}$ to $1.7\times10^{-6}\,K^{-1}$ [16,38]. No intrinsic expansion coefficients have been published for $In_2W_3O_{12}$, and no reports on the high pressure behavior of this material exist to date. In this paper we present variable temperature and high pressure X-ray diffraction studies on $In_2W_3O_{12}$, which was prepared using a non-hydrolytic sol–gel method.

2. Materials and methods

2.1. Sample preparation

Reactions were set up using standard Schlenk and glovebox techniques. All glassware was dried overnight. Starting materials were purchased from Strem Chemicals (WCl_6, 99.9%) Alfa Aesar ($InCl_3$, 99.9%), Fisher Scientific (CH_3CN), and Aldrich (iPr_2O, 99%). CH_3CN was distilled from CaH_2, all other materials were used as purchased. $InCl_3$ (2 mmol) and WCl_6 (3 mmol) were placed in a glass ampoule in the glovebox. CH_3CN (8 mL) was added to the same ampoule. The ampoule was capped with a septum, and transferred to a Schlenk line outside the glovebox. While the ampoule contents were stirring, iPr_2O (12 mmol) was added. The mixture was left to stir at room temperature for 30 min. The ampoule was then cooled in liquid N_2, and sealed under vacuum. The sealed ampoule was heated at 130 °C over a period of 7 day. It was opened in air, and the sample was recovered by evaporation. The resulting tar was heat treated to 400 °C for 3 h to convert the sample to a black powder, and then to 600 to 700 °C for 3 h to obtain crystalline material.

2.2. Characterization methods

Room temperature powder X-ray diffraction data were collected on a PANalytical X'Pert Pro diffractometer, using Cu-K_α radiation and an X'Celerator detector in Bragg Brentano geometry. Variable temperature X-ray diffraction data were acquired on a Scintag XDS-2000 equipped with a Moxtek detector and an Anton Parr high temperature stage with a platinum heater strip. Samples were mixed with silicon as an internal standard to correct for sample height offsets as a function of temperature. Data were collected over the temperature range 30 to 600 °C, with the first scan at 30 °C, and then in 50 °C increments from 50 to 600 °C. Heating rates were set at 10 °C min^{-1}, and a 5 min hold time was programmed to allow for equilibration of sample temperature. Sample composition was analyzed by energy dispersive X-ray spectroscopy on a Hitachi S-4800 scanning electron microscope using an Oxford Instruments EDS detector.

High pressure *in-situ* X-ray diffraction experiments were carried out at the Cornell High Energy Synchrotron Source (CHESS) at beam line B2 using a four post diamond anvil cell with 2.1 mm thick diamonds and 500 μm cullet faces. Samples were suspended in a 4:1 absolute methanol:ethanol mixture, which was used as the pressure-transmitting fluid. This medium remains hydrostatic up to 10.4 GPa [39]. The sample mixture was then packed inside a stainless steel gasket with a thickness and hole diameter of 100 μm and 250 μm, respectively. Ruby chips were added to allow for pressure calibration using the ruby fluorescence technique [40,41]. The wavelength used for data collection was 0.48595 Å, and the exposure time was 900 s. Data were collected on a Mar345 detector as 2D powder patterns. The sample was compressed to 7.15 GPa in ~0.3 to 0.5 GPa increments, and then decompressed to 0.49 GPa in slightly larger steps.

X-ray data were analyzed by Le Bail refinements using the FullProf software suite [42,43]. Le Bail mode was chosen to avoid discrepancies in peak intensities due to the small sample sizes used for non-ambient experiments, which often result in non-random intensities. High pressure data were integrated using Fit2D before refinement [44]. Very strong spots from large crystallites were masked before integration. For patterns corresponding to new high pressure phases, peak positions were extracted in JADE [45], and used in the indexing programs DICVOL [46], TREOR [47], and ITO [48]. A Birch–Murnaghan equation of state (EOS)[49] was fitted to the calculated unit cell volumes using the EOS-FIT program (v5.2)[50]. A third-order Birch–Murnaghan EOS was used.

3. Results and discussion

Samples of $In_2W_3O_{12}$ were recovered as dark tars after non-hydrolytic sol–gel synthesis. Crystallization was observed between 600 and 700 °C. EDS analysis gave a 2:3 ratio of In:W in all particles. Powder X-ray diffraction data collected at room temperature could be fitted with the monoclinic $P\,2_1/a$ structure previously reported for $In_2W_3O_{12}$. Variable temperature diffraction studies revealed a phase transition to the orthorhombic Pnca polymorph between 200 and 250 °C, which is in agreement with previous literature reports [24,38]. Lattice constants as a function of temperature were extracted in FullProf, and showed that both phases exhibit positive volume thermal expansion (Fig. 1). The orthorhombic phase displays anisotropic expansion, with values of $\alpha_a=-3.1\times10^{-6}\,K^{-1}$, $\alpha_b=11\times10^{-6}\,K^{-1}$, $\alpha_c=1.6\times10^{-6}\,K^{-1}$, resulting in an average linear expansion coefficient α_l of $3.1\times10^{-6}\,K^{-1}$. This value is higher than those previously reported from dilatometer measurements [16,38]. However, dilatometry cannot distinguish intrinsic and extrinsic contributions to expansion, and it is unknown whether the measured specimens contained randomly oriented particles.

High pressure data for $In_2W_3O_{12}$ were collected at room temperature up to 7.1 GPa. One phase transition was observed before irreversible amorphization occurred (Fig. 2). Le Bail refinement of the initial X-ray pattern in space group $P\,2_1/a$ gave an excellent fit (Fig. 3). The extracted lattice constants, $a=16.403$ Å, $b=9.630$ Å, $c=19.020$ Å and $\beta=125.53°$, are similar to those obtained under ambient conditions. This monoclinic cell could

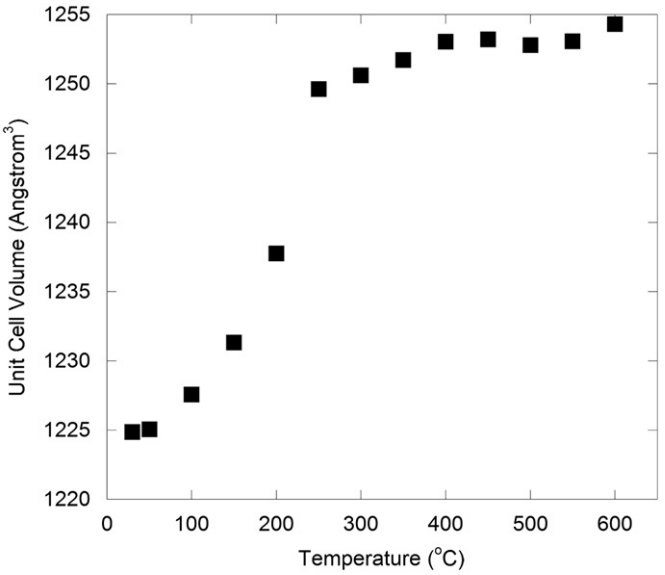

Fig. 1. Volume expansion of $In_2W_3O_{12}$ from variable temperature powder diffraction study.

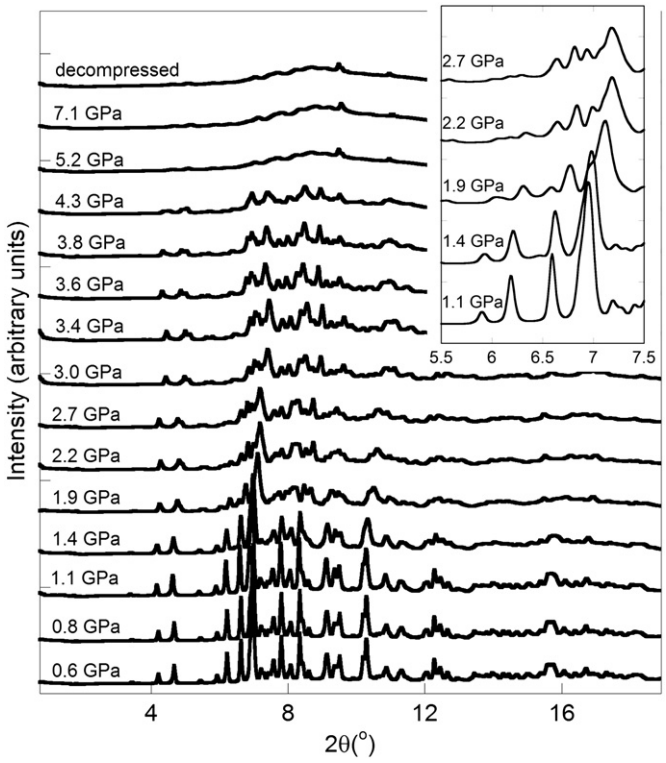

Fig. 2. Variable pressure XRD patterns for $In_2W_3O_{12}$. The insert shows that a phase transition occurs between 2.2 and 2.7 GPa.

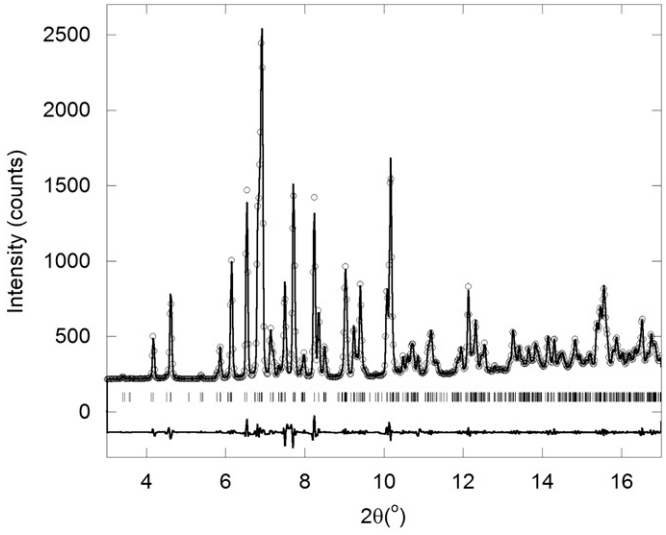

Fig. 3. Le Bail fit for the ambient pressure data set of $In_2W_3O_{12}$. The red dots represent data points, the solid line corresponds to the calculated pattern, and tick marks indicate peak positions of $In_2W_3O_{12}$. A difference plot is shown below the pattern.

account for all data below 2.2 GPa (Table 1), while a deterioration in fit quality was observed at 2.2 GPa, suggesting a possible phase transition. Close inspection of the data (Fig. 2 inset) revealed the onset of this phase transition already in the 1.9 GPa dataset, and coexistence of the two phases is clearly observed at 1.9 and 2.2 GPa. This is most obvious from inspection of the region between 6 and 6.5° 2θ. The peaks at 6° and 6.5° belong to the low and high pressure phases, respectively. Both peaks are observed in the 1.9 and 2.2 GPa data, while only one is present at lower or higher pressures. The phase transition was further verified by the less than satisfactory fit of the 2.7 GPa data using the monoclinic $P\,2_1/a$ cell (Fig. 4(a)). This new phase was present

Table 1
$In_2W_3O_{12}$ lattice constants and unit-cell volume as a function of pressure determined by Le Bail fits.

P (GPa)	Chi^2	R_f	a (Å)	b (Å)	c (Å)	β(°)	Volume (Å^3)
Ambient	0.22	0.05	16.403	9.630	19.020	125.53	2445.1
0.6	0.19	0.04	16.249	9.517	18.740	125.62	2355.7
0.8	0.24	0.03	16.227	9.509	18.721	125.62	2348.6
1.1	0.18	0.02	16.145	9.458	18.631	125.68	2310.9
1.4	0.21	0.03	16.056	9.433	18.507	125.72	2275.9
1.9	0.33	0.10	15.952	9.491	18.309	125.96	2243.7
2.2	0.23	0.14	15.951	9.522	18.181	126.01	2233.7
2.7	0.42	0.15	19.679	4.491	17.341	99.21	1512.7
3.0	0.33	0.31	19.509	4.473	17.259	99.04	1487.5
3.4	0.47	0.61	19.407	4.446	17.156	99.08	1461.8
3.6	0.38	0.34	19.380	4.430	17.065	98.99	1446.9
3.8	0.33	0.36	19.310	4.419	17.017	98.99	1434.2

until about 4.3 GPa, at which pressure the onset of partial amorphization was observed.

Indexing attempts using peak positions extracted for the 2.7 GPa dataset did not give any reasonable cells. One possible explanation for this is that the two phases could still coexist at this pressure, or that peak overlap results in inaccurate peak position extraction. Datasets collected at higher pressures did not allow extraction of enough high quality peak positions for reliable indexing. Comparison of the patterns to other high pressure diffraction patterns reported in the literature revealed similarities to published patterns for $Sc_2W_3O_{12}$, $Al_2W_3O_{12}$, and $Sc_2Mo_3O_{12}$ [34,35,37,51]. These orthorhombic compounds were found to transform to the monoclinic $P\,2_1/a$ polymorph at very low pressures (0.1 to 0.6 GPa), and underwent a second crystalline-to-crystalline phase transition at pressures between 3.2 and 3.5 GPa to a phase that gave similar powder patterns to $In_2W_3O_{12}$ at 2.7 GPa. This high pressure phase was also observed for $Ga_2Mo_3O_{12}$ at pressures above 2.4 GPa [21]. Phase coexistence of the higher pressure phase and the monoclinic $P\,2_1/a$ polymorph were reported for $Sc_2W_3O_{12}$ between 1.6 and 3.0 GPa, similar to what was observed in this study [51]. No indexing results are available for $Sc_2Mo_3O_{12}$, but lattice constants for $Al_2W_3O_{12}$, $Sc_2W_3O_{12}$, and $Ga_2Mo_3O_{12}$ have been reported. These lattice constants were used as starting points for Le Bail refinements in space group $P\,2$ for $In_2W_3O_{12}$. While the published lattice constants did not give excellent fits, the fit quality was convincing enough to suggest that $Al_2W_3O_{12}$, $Sc_2W_3O_{12}$, $Ga_2Mo_3O_{12}$ and $In_2W_3O_{12}$ adopt the same high pressure structure. Initial indexing on $Ga_2Mo_3O_{12}$, which was previously carried out in our group, yielded several reasonable cells with comparable statistics. Based on minor differences in fit quality, the cell reported in the literature was chosen. However, the $Ga_2Mo_3O_{12}$ sample investigated contained a MoO_3 impurity phase, which could have affected the cell choice. All reasonable cells previously obtained for $Ga_2Mo_3O_{12}$ were used for Le Bail refinements. While none of the cells could account for all of the peaks, a cell with lattice constants of $a=19.675$ Å, $b=4.491$ Å, $c=17.341$ Å and $\beta=99.21°$ gave the best fit (Fig. 4(b)). The discrepancies observed could be a result of small amounts of impurity phases, including residual $P\,2_1/a$ polymorph. Le Bail fits using the alternative high pressure phase cell were significantly better than fits using the lower pressure $P\,2_1/a$ cell. This smaller monoclinic cell could account for the data up to 4.3 GPa, at which pressure partial amorphization occurred. This is very similar to the pressure at which the onset of amorphization was observed in $Sc_2W_3O_{12}$ (4.2 GPa). The amorphous phase was retained during decompression.

The extracted unit cell volumes as a function of pressure show an abrupt volume change of ~32% at the transition pressure. This suggests that the high pressure phase used to fit the data must

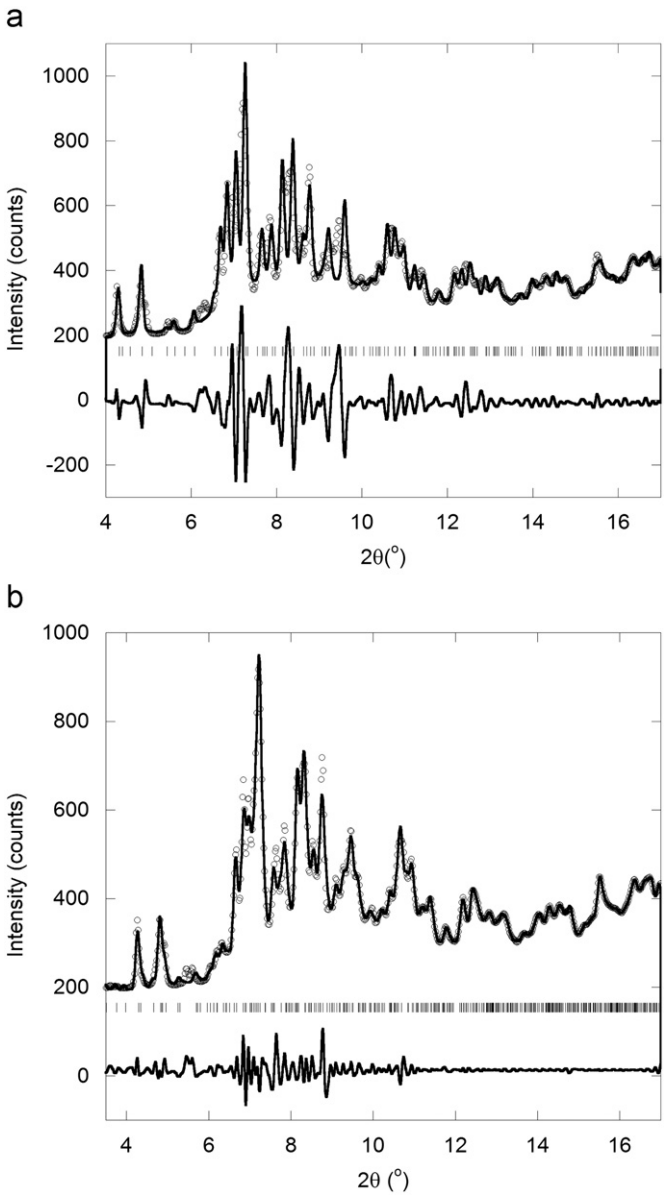

Fig. 4. Le Bail fit of the 2.7 GPa data for $In_2W_3O_{12}$ (a) using the *P 2₁/a* monoclinic cell observed for lower pressures, and (b) a smaller monoclinic cell with $a=19.675$ Å, $b=4.491$ Å, $c=17.341$ Å and $\beta=99.21^\circ$.

contain a smaller number of formula units (Z). The volume per formula unit at 2.2 GPa ($Z=8$) is $\sim$280 Å^3. An identical volume per formula unit at 2.7 GPa would correspond to 5.4 formula units, suggesting that the high pressure phase may contain six formula units per cell, with a volume of $\sim$250 Å^3 each. This would correspond to a decrease in unit cell volume per formula unit of $\sim$10% at the phase transition (Fig. 5), which is comparable to commonly observed volume decreases at pressure induced phase transitions [37,52,53]. While a Z of six is possible in a monoclinic cell, it is also possible that the cell used for refinements is a sub- or supercell of the true unit cell.

The compressibility of the two $In_2W_3O_{12}$ phases was calculated from the extracted lattice constants. The volume compressibility, β_v, of the initial monoclinic phase of $In_2W_3O_{12}$ was -4.3×10^{-2} GPa^{-1}. The linear compressibilities for a, b and c were -1.5×10^{-2} GPa^{-1}, -8.3×10^{-3} GPa^{-1}, and -1.8×10^{-2} GPa^{-1}, respectively. The compressibilities of the a and c axes are similar, but the *b* axis shows a smaller value. This is in agreement with previous literature reports stating that $A_2M_3O_{12}$ compounds

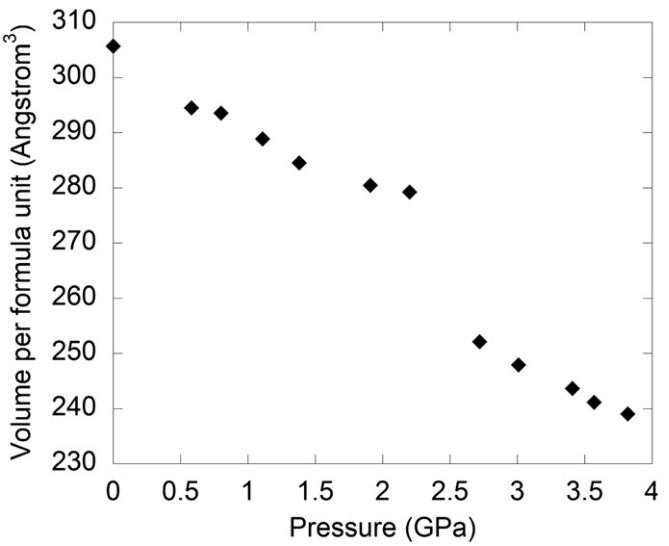

Fig. 5. Change in unit cell volume per formula unit as a function of pressure for $In_2W_3O_{12}$. V/Z for the high pressure phase was calculated assuming $Z=6$.

show anisotropic compressibility, with the *b* axis being stiffer [35]. The high pressure phase gave volume and linear compressibilities of -4.8×10^{-2} GPa^{-1}, -1.6×10^{-2} GPa^{-1}, -1.5×10^{-2} GPa^{-1} and -1.8×10^{-2} GPa^{-1}, respectively. In contrast to the initial monoclinic phase, the compressibilities of all three axes are very similar. It is interesting to note that the high pressure phase is slightly more compressible than the ambient pressure monoclinic phase. Similar behavior has been observed for the orthorhombic *Pnca* and monoclinic *P 2₁/a* polymorphs in several materials [35,36].

A third order Birch–Murnaghan EOS fit to the extracted unit cell volumes for the low pressure monoclinic phase gave a bulk modulus K_0 of 13(2) GPa, and a zero pressure volume of 305.6 Å^3 pre formula unit. These values are comparable to those reported for $Sc_2Mo_3O_{12}$ and $Sc_2W_3O_{12}$ [34,35].

The reversibility of the crystalline to crystalline phase transition was not addressed, as the sample was further compressed, and started to amorphize above 4 GPa. No changes were detected during decompression, indicating that the amorphization was irreversible.

4. Conclusions

In situ high temperature and pressure diffraction studies on $In_2W_3O_{12}$ have shown that this compound is not the best candidate for controlled thermal expansion composites, as it only exhibits uniaxial negative thermal expansion, and overall positive volume expansion. In addition, the occurrence of a pressure induced phase transition between 1.9 and 2.7 GPa could be problematic during composite processing. The phase transition is accompanied by a compressibility collapse, resulting in higher compressibility of the denser high pressure polymorph. This is similar to observations in other compounds in the $Sc_2W_3O_{12}$ family. The origin of this intriguing behavior is unclear, and warrants further experimental and theoretical work.

Acknowledgments

This research was funded by the National Science Foundation under grant DMR-0545517 and 0840474. The high pressure studies were conducted at the Cornell High Energy Synchrotron Source (CHESS) which is supported by the National Science Foundation and

the National Institutes of Health/National Institute of General Medical Sciences under NSF award DMR-0936384. We are grateful to Dr. Zhongwu Wang for his help with the cell set-up.

Appendix A. Supplementary materials

Supplementary materials associated with this article can be found in the online version at doi:10.1016/j.jssc.2012.01.019.

References

[1] T. Suzuki, A. Omote, J. Am. Ceram. Soc. 87 (2004) 1365–1367.
[2] K.W. Chapman, P.J. Chupas, C.J. Kepert, J. Am. Chem. Soc. 127 (2005) 15630–15636.
[3] J.S.O. Evans, P.A. Hanson, R.M. Ibberson, N. Duan, U. Kameswari, A.W. Sleight, J. Am. Chem. Soc. 122 (2000) 8694–8699.
[4] G. Ernst, C. Broholm, G.R. Kowach, A.P. Ramirez, Nature 396 (1998) 147–149.
[5] L.P. Huang, J. Kieffer, Phys. Rev. Lett. 95 (2005).
[6] R. Mittal, S.L. Chaplot, H. Schober, T.A. Mary, Phys. Rev. Lett. 86 (2001) 4692–4695.
[7] A.P. Ramirez, G.R. Kowach, Phys. Rev. Lett. 80 (1998) 4903–4906.
[8] M.G. Tucker, A.L. Goodwin, M.T. Dove, D.A. Keen, S.A. Wells, J.S.O. Evans, Phys. Rev. Lett. 95 (2005).
[9] J.S.O. Evans, Z. Hu, J.D. Jorgensen, D.N. Argyriou, S. Short, A.W. Sleight, Science 275 (1997) 61–65.
[10] A.L. Goodwin, M. Calleja, M.J. Conterio, M.T. Dove, J.S.O. Evans, D.A. Keen, L. Peters, M.G. Tucker, Science 319 (2008) 794–797.
[11] T.A. Mary, J.S.O. Evans, T. Vogt, A.W. Sleight, Science 272 (1996) 90–92.
[12] C.A. Perottoni, J.A.H. da Jornada, Science 280 (1998) 886–889.
[13] A.W. Sleight, Annu. Rev. Mater. Sci. 28 (1998) 29–43.
[14] A.W. Sleight, Curr. Opin. Solid State Mater. Sci. 3 (1998) 128–131.
[15] A.W. Sleight, Inorg. Chem. 37 (1998) 2854–2860.
[16] T.A. Mary, A.W. Sleight, J. Mater. Res. 14 (1999) 912–915.
[17] J.S.O. Evans, T.A. Mary, A.W. Sleight, J. Solid State Chem. 133 (1997) 580–583.
[18] J.S.O. Evans, T.A. Mary, Int. J. Inorg. Mater. 2 (2000) 143–151.
[19] P.M. Forster, A.W. Sleight, Int. J. Inorg. Mater. 1 (1999) 123–127.
[20] P.M. Forster, A. Yokochi, A.W. Sleight, J. Solid State Chem. 140 (1998) 157–158.
[21] S.D. Gates, J.A. Colin, C. Lind, J. Mater. Chem. 16 (2006) 4214–4219.
[22] K. Nassau, H.J. Levinstein, G.M. Loiacono, J. Phys. Chem. Solids 26 (1965) 1805–1816.
[23] K. Nassau, J.W. Shiever, E.T. Keve, J. Solid State Chem. 3 (1971) 411–419.
[24] A.W. Sleight, L.H. Brixner, J. Solid State Chem. 7 (1973) 172–174.
[25] S. Sumithra, A.K. Tyagi, A.M. Umarji, Mater. Sci. Eng. B 116 (2005) 14–18.
[26] S. Sumithra, A.M. Umarji, Solid State Sci. 8 (2006) 1453–1458.
[27] D.K. Balch, D.C. Dunand, Metall, Mater. Trans. A 35A (2004) 1159–1165.
[28] H. Holzer, D.C. Dunand, J. Mater. Res. 14 (1999) 780–789.
[29] C. Verdon, D.C. Dunand, Scr. Mater. 36 (1997) 1075–1080.
[30] J.D. Jorgensen, Z. Hu, S. Short, A.W. Sleight, J.S.O. Evans, J. Appl. Phys. 89 (2001) 3184–3188.
[31] B. Chen, D.V.S. Muthu, Z.X. Liu, A.W. Sleight, M.B. Kruger, Phys. Rev. B 64 (2001).
[32] Z. Hu, J.D. Jorgensen, S. Teslic, S. Short, D.N. Argyriou, J.S.O. Evans, A.W. Sleight, Physica B 241 (1997) 370–372.
[33] M. Maczka, W. Paraguassu, A.G. Souza, P.T.C. Freire, J. Mendes, F.E.A. Melo, J. Hanuza, J. Solid State Chem. 177 (2004) 2002–2006.
[34] T. Varga, A.P. Wilkinson, C. Lind, W.A. Bassett, C. Zha, Phys. Rev. B 71 (2005) 214106.
[35] T. Varga, A.P. Wilkinson, C. Lind, W.A. Bassett, C. Zha, J. Phys. Condens. Matter 17 (2005) 4271–4283.
[36] M. Cetinkol, A.P. Wilkinson, Phys. Rev. B 79 (2009) 224118.
[37] G.D. Mukherjee, V. Vijaykumar, S.N. Achary, A.K. Tyagi, B.K. Godwal, J. Phys. Condens. Matter 16 (2004) 7321–7330.
[38] V. Sivasubramanian, T.R. Ravindran, R. Nithya, A.K. Arora, J. Appl. Phys. 96 (2004) 387–392.
[39] R.A. Miletich, W.F. Kuhs, High Temp.High Press. Cryst. Chem. 41 (2000) 445–519.
[40] H.K. Mao, P.M. Bell, J.W. Shaner, D.J. Steinberg, J. Appl. Phys. 49 (1978) 3276–3283.
[41] J.D. Barnett, S. Block, J.G. Piermarini, Rev. Sci. Instrum 44 (1973) 1.
[42] A. Le Bail, H. Duroy, J.L. Fourquet, Mater. Res. Bull. 23 (1988) 447–452.
[43] J. Rodriguez-Carvajal, in FULLPROF: A Program for Rietveld Refinement and Pattern Matching Analysis, Satellite Meeting on Powder Diffraction of the XV Congress of the IUCr, Toulouse, France, 1990; p. 127.
[44] A.P. Hammersley, Fit2D: An Introduction and Overview, ESRF, Grenoble Cedex, France, 1997.
[45] JADE, Materials Data Inc., Livermore, CA.
[46] D. Louer, A. Boultif, (1992) Dicvol91.
[47] P.E. Werner, L. Erikkson, J. Appl. Crystallogr. 18 (1990) 367–370.
[48] J.W. Visser, J. Appl. Crystallogr. 2 (1969) 89–95.
[49] F. Birch, Phys. Rev. 71 (1947) 809.
[50] R.J. Angel, Computer Code EOS-FIT, v. 5.2, Virginia Tech, Blacksburg, VA, 2001.
[51] N. Garg, C. Murli, A.K. Tyagi, S.M. Sharma, Phys. Rev. B 72 (2005) 064106.
[52] C. Lind, D.G. VanDerveer, A.P. Wilkinson, J.H. Chen, M.T. Vaughan, D.J. Weidner, Chem. Mater. 13 (2001) 487–490.
[53] C.A. d.J. Perottoni, J. A. H, Science 80 (1998) 886.